Int J Earth Sci (Geol Rundsch) (2017) 106:2727–2746
DOI 10.1007/s00531-017-1456-y

ORIGINAL PAPER

Geochronological data of igneous and metamorphic rocks from the Xing'an-Mongolia Orogenic Belt of the eastern Central Asian Orogenic Belt: implications for the final closure of the Paleo-Asian Ocean

Wang Guosheng[1] · Wu Chen[1] · Chen Cheng[2] · Zhou Zhiguang[1] · Liu Changfeng[1] · Jiang Tian[1]

Received: 18 October 2016 / Accepted: 1 February 2017 / Published online: 4 March 2017

Abstract In order to better constrain the evolution of the Xing'an-Mongolia Orogenic Belt and the resulting closure of the Paleo-Asian Ocean, we conducted an integrated investigation involving U-Pb dating of igneous and detrital zircon and a synthesis of existing work across the Erdaojing and Ondor Sum complexes in the eastern segment of the Central Asian Orogenic Belt. Geochronological analysis revealed a different tectonic setting between the Ondor Sum complex (Tulinkai area) and the Erdaojing accretion complex, as detrital zircon U-Pb analysis identified different major age provenances: (1) the Precambrian basement of the North China Craton and Paleozoic Bainaimiao Arc along the northern margin of North China to the south are the provenance rocks of the schists in the Tulinkai area, and (2) the Precambrian basement of the Xilinhot complex and Paleozoic Baolidao arc to the north are the provenance rocks of the schists in the Erdaojing area. We infer that the existence of the ocean between the above two regions in the late of Early Paleozoic in accordance with the result of this study. Furthermore, a comparison of the youngest age population in the intruded-diorite rock and metasedimentary rocks with U-Pb ages implies that the final closure of the Paleo- Asian Ocean along the Solonker Suture Zone most likely occurred in the period between 239 and 222 Ma (Late Paleozoic-Triassic).

Keywords Ondor Sum complex · Erdaojing complex · Paleo-Asian Ocean · Xing'an-Mongolia Orogenic Belt · Late Paleozoic-Triassic

Introduction

The Central Asian Orogenic Belt (CAOB) is one of the largest Phanerozoic orogenic systems on Earth (Cawood et al. 2009) (Fig. 1), which is generally thought to separate the North China Craton from the growing accretionary front encircling the Siberian Craton (e.g., Jahn et al. 2000, 2004; Windley et al. 2007; Xiao et al. 2003, 2009a, b, 2010, 2013, 2015; Kröner et al. 2007; Song et al. 2015). This area has attracted much attention from researchers in the last decade, as its formation is related to accretionary processes (e.g., accretion of terranes, accretionary wedges, seamounts, subduction roll-back and back-arc basin opening and closure) and continental crust formation induced by the Palaeozoic subduction of the Palaeo-Asian Ocean that had evolved for a long period of time since the Neoproterozoic (e.g., Şengör et al. 1993; Xiao et al. 2003, 2009a, b; Windley et al. 2007; Wang et al. 2009; Zhang et al. 2009a,

Electronic supplementary material The online version of this article (doi:10.1007/s00531-017-1456-y) contains supplementary material, which is available to authorized users.

✉ Wang Guosheng
wanggsh@cugb.edu.cn

Wu Chen
wuchen2016@cugb.edu.cn

Chen Cheng
Xiaobaicongxi@126.com

Zhou Zhiguang
zhouzhg@cugb.edu.cn

Liu Changfeng
nose010@sohu.com

Jiang Tian
jiangtian71@gmail.com

[1] School of Earth Science and Resources, China University of Geosciences (Beijing), Beijing 100083, China

[2] Sichuan Institute of Geological Engineering Investgation, Chengdu 610072, China

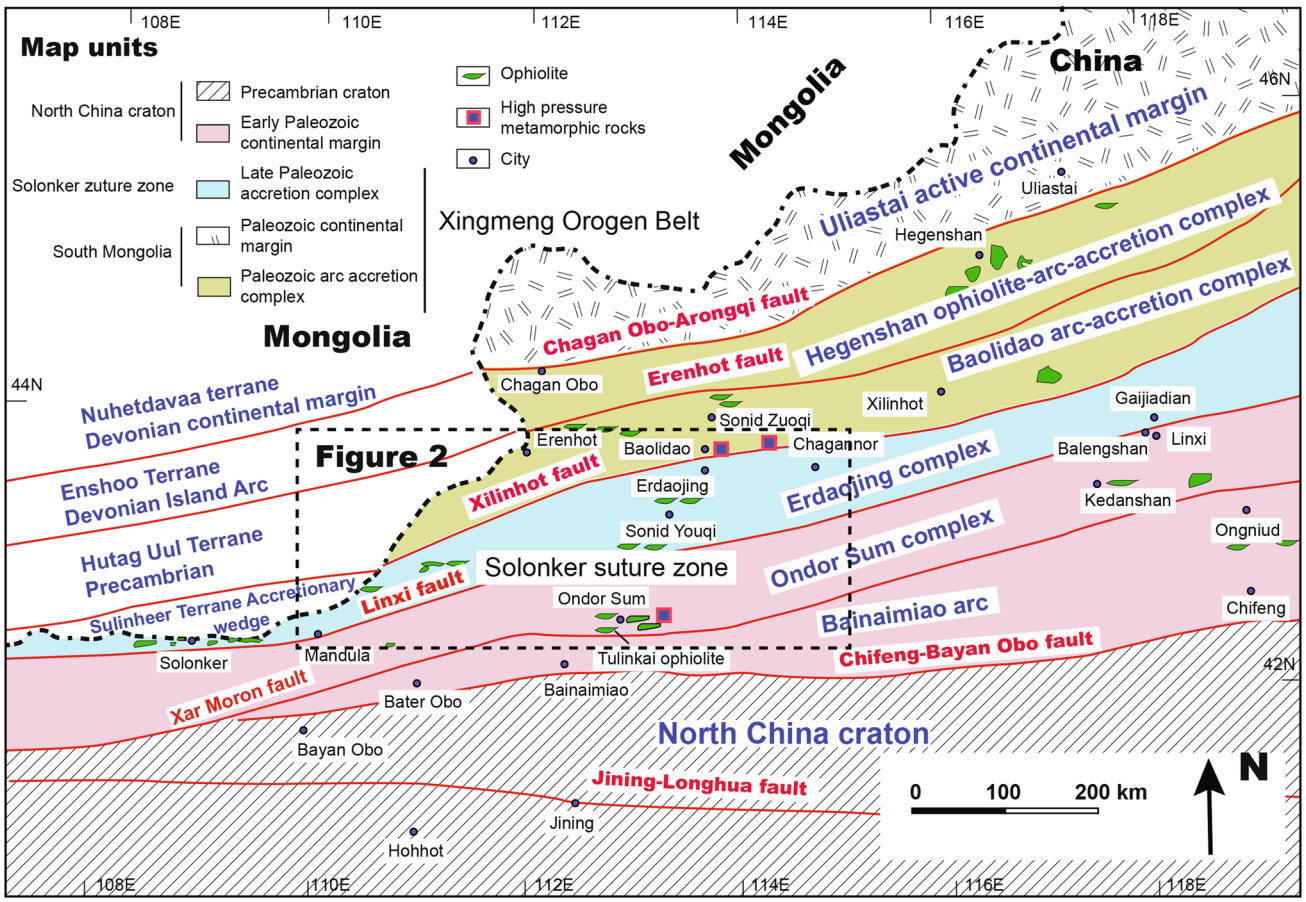

Fig. 1 Sketch map of the geology in the southern Central Asian Orogenic Belt, modified from Xiao et al. (2003) and Wu et al. (2016) based on our own observations showing the Solonker suture zone separating the northern and southern Paleozoic orogens. The *blue dash box* shows the location of the study area

b, c; Eizenhöfer et al. 2015; Liu et al. 2016) (Fig. 1). Final disappearance of the Paleo-Asian Ocean between the North China and Siberian Cratons terminated the formation of the CAOB, leading to collision between the combined North China Craton and the southern accretionary margin of the Siberian Craton in the Late Paleozoic and/or Early Mesozoic time (e.g., Xiao et al. 2009a, b, 2015; Liu et al. 2012; Eizenhöfer et al. 2014; Xu et al. 2015; Song et al. 2015; Li et al. 2016a, b). However, several issues dealing with the Paleozoic evolution of the Paleo-Asian Ocean remain speculative, especially the location of suture zone and the timing of the final oceanic closure.

Several tectonic models have been proposed to explain the formation and evolution of the CAOB, The end-member models include: (1) single-arc model of Şengör et al. (1993), which requires main elements of the CAOB were derived from a single (or multiple of Yakubchuk 2008) ocean spanning arc system, (2) archipelago-type tectonic model of Xiao et al. (2003, 2009a, b, 2010), Windley et al. (2007), and Lehmann et al. (2010), which predicts that distinct volcanic arcs and blocks were accreted onto the active margins of the Siberian Craton from the Early Paleozoic to the Early Mesozoic. Also, several subdivision schemes in terms of the tectonic architecture of the eastern part of the CAOB had been proposed (e.g., Wang and Liu 1986; Chen et al. 2000; Badarch et al. 2002; Xiao et al. 2003, 2009a, 2015; Xu et al. 2013, 2014, 2015; Eizenhöfer et al. 2014, 2015; Song et al. 2015; Zhang et al. 2015), which made the relationship between major tectonic blocks confusing to understand.

A more detailed understanding is needed with respect to the development of volcanic arcs, the relative paleogeographic location of terranes before the final closure, and the interaction between respective tectonic elements within the Paleo-Asian Ocean. Detrital U-Pb zircon geochronology of Paleozoic sedimentary arc basins is a potentially powerful tool with which to quantitatively evaluate issues of when and how opening and closing of the ocean. It provides information on relationships between major tectonic blocks, such as their relative paleogeographic locations in

time or contribution to sedimentary material (Haughton et al. 1991). Major tectonic units can be identified by comparing age distributions to well-defined "age-fingerprints" of likely provenance terrane candidates.

Xing'an-Mongolia Orogenic Belt of the eastern Central Asian Orogenic Belt is characterized by various Phanerozoic accretionary orogen, which are interpreted as island arcs, forearc or back-arc basins, ophiolites, and microcontinents (e.g., Şengör et al. 1993; Xiao et al. 2003, 2009a, b, 2013; Windley et al. 2007; Eizenhöfer et al. 2015; Song et al. 2015; Xu et al. 2015; Zhang et al. 2015) (Fig. 1). This work evaluates the location and timing of the final closure of the Paleo-Asian Ocean, and identifies major sedimentary provenance terranes within the Xing'an-Mongolia Orogenic Belt. The main goal of this paper is to use coupled U-Pb dating of detrital zircon to determine zircon-population distributions in the Erdaojing and Ondor Sum complexes of central Inner Mongolia (Fig. 2). The detrital-zircon-grain ages record the crystallization of the source rock and can only place a maximum age on deposition of the host strata, and that detrital zircons are highly susceptible to sedimentary recycling given their resistance to mechanical abrasion. In additional, our U-Pb detrital zircon dating provides valuable information about the provenance of the metasedimentary rocks in the Xing'an-Mongolia Orogenic Belt. Comparison of zircon populations in the study area and those of bedrock allows us to quantify the spatial relationships of zircon populations between the Erdaojing and Ondor Sum complexes and the processes that transfer zircon populations from the source regions to the forearc basin.

Regional geology

The eastern section of the CAOB is characterized by east–northeast trending tectonic units, consisting of ophiolites, arcs, accretionary wedges and associated

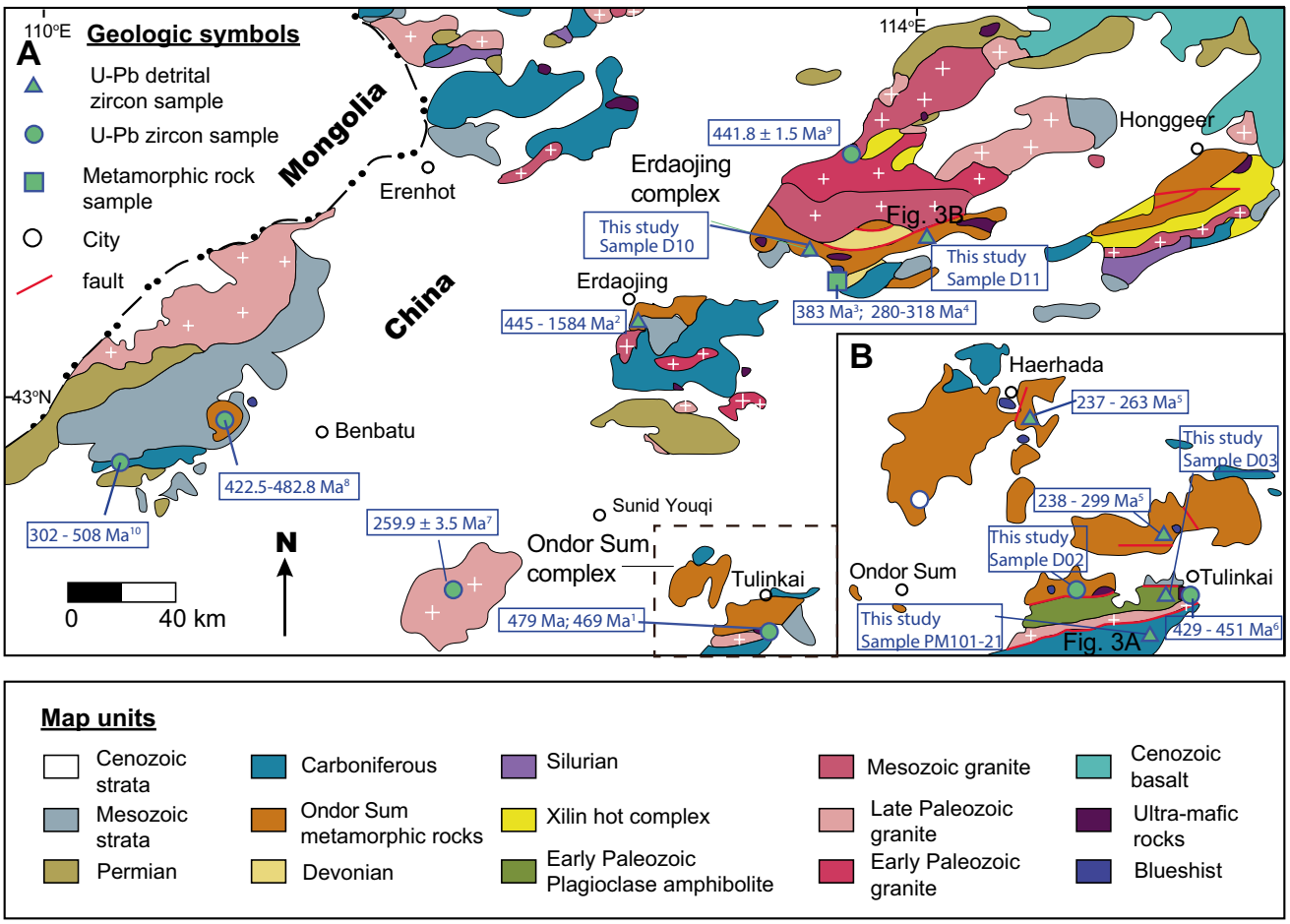

Fig. 2 Simplified geological map of the study area, modified from Chu et al. (2013) based on our own observations, showing sample localities. Ages data from: (1) Jian et al. (2008); (2) Li et al. (2012); (3) Xu et al. (2014); (4) Chen et al. (2009); (5) Chu et al. (2013); (6) Liu et al. (2003); (7) Liu et al. (2015); (8) Wu et al. (2016); (9) Li et al. (2016); (10) Zhou et al. (2009)

volcanosedimentary rocks that were assembled during the final Late Paleozoic–Early Mesozoic closure of the Paleo-Asian Ocean (e.g., Sengör et al. 1993; Ye et al. 1994; Xiao et al. 2010; Wu et al. 2014, 2015; Zhang et al. 2015) (Fig. 1). The eastern section of the CAOB region can be divided into three domains, from north to south (Fig. 1): the accretionary zone between the Solonker suture and the Uliastai continental margin, the Solonker suture zone, and the southern accretionary zone between the North China Craton and the Solonker suture (Xiao et al. 2003, 2009a, b; Xu et al. 2013). The northern accretionary zone extends southward from a continental margin that was active during Devonian to Carboniferous times, through the Hegenshan ophiolitic accretionary complex to the Late Carboniferous Baolidao arc (Xiao et al. 2003; Li et al. 2014) (Fig. 1). The southern accretionary zone is characterized by the Middle Ordovician–early Silurian Ondor Sum subduction–accretion complex (De Jong et al. 2006; Jian et al. 2008) and the Bainaimiao arc (Fig. 1). Complete subduction of the Paleo-Asian Ocean caused the two opposing active continental margins to collide, leading to formation of the Solonker suture (Xiao et al. 2003). Whether the Solonker Suture Zone was formed by episodic (Jian et al. 2008, 2010) or continuous (Chen et al. 2000, 2009; Xiao et al. 2003) tectonic activity caused by subduction of oceanic lithosphere is also debated. According to the published models proposed by Li et al. (2006) and Jian et al. (2008, 2010), the Solonker Suture Zone is located along the northern bank of the Xar Moron River. Most researchers (e.g., Wu et al. 2002, 2007; Xiao et al. 2003; De Jong et al. 2006; Li et al. 2006; Shen et al. 2006; Zhang et al. 2007, 2009a, b, c; Jian et al. 2008, 2010; Lin et al. 2008; Chen et al. 2009; Eizenhöfer et al. 2014, 2015) locate the final closure of the Paleo-Asian Ocean along the banks of the Xar Moron River. However, some other authors (e.g., Shao 1989; Tang 1990; Nozaka and Liu 2002) assume that the final collision took place further north near the Hegenshan Ophiolite Complex (see Miao et al. 2008) varying from end of the Devonian to the Middle Mesozoic. Inner Mongolia is an accretionary orogen that has one terminal suture zone passing through Solonker, which contains many lenses of melange, ophiolites and blueschists (Xiao et al. 2003).

The Northeast China, tectonically named in the past as Xing'an-Mongolian Orogenic Belt, geosyncline or fold system (IMBGMR 1991) and Manchurides of Sengör and Natal'in (1996), composes the main part of the eastern segment of the CAOB, and tectonically located in the area surrounded by the Siberian Craton to the north, the North China Craton to the south and the western Pacific Plate to the east. The tectonic evolution in the area was closely related to the Paleo-Asian Ocean and Paleo-Pacific Ocean regimes during the Paleozoic-Early Mesozoic (e.g., Li et al. 2006; Windley et al. 2007; Xiao et al. 2003, 2009a, b, 2015). Li et al. (2006) considered that there are two kinds of different tectonic domains in NE China and its surrounding areas, i.e. Pre-Sinian blocks or massifs with the Archean-Paleoproterozoic or Middle Proterozoic-Early Neoproterozoic basements and the Phanerozoic orogenic belts of various ages, based on which he divided the NE China from west to east into Central Mongolian-Ergun blocks, South Mongolian-Central Great Xing'an orogenic belt and Bureya-Jiamusi paleoplate. Recently, Xu et al. (2015) gave a tectonic division of the Xing'an-Mongolia Orogenic Belt according to tectonics, geochronology and geochemistry. They recognized four blocks and four sutures in the Xing'an-Mongolia Orogenic Belt, including the Erguna block, Xing'an-Airgin Sum block, Songliao-Hunshandake block and Jiamusi block, and Xinlin-Xiguitu suture, Xilinhot-Heihe suture, Mudanjiang suture and Ondor Sum-Yanji suture. Liu et al. (2016) suggest that the Paleozoic tectonic divisions in Northeast China are, from west to east, Erguna block, Xing'an block, Songliao-Xilinhot block and Jiamusi block, and Xinlin-Xiguitu suture, Heihe-Hegenshan suture, Mudanjiang-Yilan suture between them and Solonker-Xar Moron-Changchun-Yanji suture between the blocks in the Northeast China and North China Craton to the south.

The basement of the North China Craton consists of Archaean and Lower Proterozoic rocks, covered by passive margin sediments of Neoproterozoic to early Paleozoic age (Hsü et al. 1991). On the northern side of the Chifeng-Bayan Obo fault is the Mid-Ordovician to Early Silurian Bianaimiao arc (Hu et al. 1990), which comprises calc-alkaline tholeiitic basalts to minor felsic lavas, alkaline basalts, and agglomerates, volcanic breccias, tuffs, granodiorites, and granites (e.g., Xiao et al. 2003). There is no evidence of subduction zone rocks or a suture zone south of Bainaimiao regional to allow northward subduction to create this arc, and therefore Xiao et al. (2003) suggested that southward subduction was relatively responsible. The occurrence of shallow marine clastic sediments and carbonates on top of early Paleozoic granites in the western Ondor Sum region (Wang and Liu 1986) constrains the exhumation of the Bainaimiao-type magmatic rocks, which may point to the extinction of the arc. In the Silurian, Devonian and Carboniferous no island arcs were generated and accreted to the northern margin of the North China Craton (e.g., Xiao et al. 2003; De Jong et al. 2006).

Isolated outcrops of ophiolites occur around Ondor Sum, in an area of about 70 km along strike associated with high-pressure metamorphic rocks, and further eastward in the area of Kedanshan and along the northern banks of the Xar Moron River (e.g., Xiao et al. 2003; De Jong et al. 2006) (Fig. 1). The Ondor Sum complex consists of Early Paleozoic metamorphic rocks, unconformably overlain by Late Paleozoic Carboniferous sedimentary rocks and Permian volcanic-sedimentary rocks. The Ondor Sum

metamorphic rocks consist of schist and quartzite with marble lenses, which have been thrust onto the continental margin of the North China Craton. The Mesoproterozoic amphibolite-facies orthogneisses and supracrustal rocks as well as Neoproterozoic greenstones described by Zhai et al. (2003) probably belong to the basement of Ondor Sum. They are overlain by Carboniferous limestone, and Permian flysch, andesite, dolerite, sandstone, and limestone with a large number of brachiopod fossils. The original rocks of the Ondor Sum complex assemblage north of the Xar Moron fault have been intensely shredded by tectonic processes partly during accretion, and partly during subduction and exhumation (e.g., Xiao et al. 2003). There are plutonic rocks in this region with a wide compositional range and a very wide age range, which are composed of Cambrian–Ordovician granitoids, Permian diorite, quartz diorite, granodiorite (Zhou et al. 2009).

The Solonker suture zone is marked by a belt of melanges, blueschists and ophiolites that is 700 km long and 60 km wide. It contains blocks of dolomite, quartzite, mafic and ultramafic rocks, marble and blueschist (e.g., Tang 1990; Xu et al. 2001; Xiao et al. 2003; Jian et al. 2008, 2012). The accretionary wedge Erdaojing complex (Fig. 1) is composed of tectonic melange typical of a modern accretionary wedge (Tang 1990). Also, The Erdaojing accretion complex contains the youngest ophiolites among eastern CAOB. The northward younging in the ophiolitic melanges from the Early Paleozoic ophiolites in the south to the Permian ophiolites in the north, together with the fact that both these ophiolites were imbricated with the Lower Permian sediments (Li 1986, 1987), Xiao et al. (2003) suggests that the whole section represents a northward growing accretionary complex which may have been resulted from seaward retreat (northward) of a south dipping trench along which the Paleo-Asian ocean was subducted beneath the North China Craton in the Late Paleozoic. There is a substantial body of evidence indicating that the final suturing of the Solonker zone occurred between the Late Permian and earliest Triassic (Xiao et al. 2003, 2009a, b; Miao et al. 2008; Jian et al. 2010; Li et al. 2011), which may be related to the closure of the Permian oceanic basin in western Inner Mongolia (Li et al. 2011, 2014).

The Xilinhot complex is an amphibolite facies tectonic unit within the eastern part of the CAOB (Shi et al. 2003; Li et al. 2016a, b). It is distributed discontinuously as variably sized tectonic blocks in the Late Carboniferous Baolidao arc accretionary zone (IMBGMR 1991; Shi et al. 2003; Li et al. 2016a, b). The Xilinhot complex occurs within the northern accretionary zone along the northern margin of the Xilinhot fault and is well exposed at Baiyintala, Xiretu, Baiyinxile and Baiyinchagan in a region just south of Xilinhot City (IMBGMR 1991; Li et al. 2016a, b) (Fig. 1). It is in fault contact with the upper Silurian sedimentary Xuniwusu Formation to the south, which formed in a shelf environment. The complex is locally covered by volcano-sedimentary rocks above an angular unconformity. Many Late Paleozoic to Mesozoic granites and numerous later granitic and quartz veins intruded the complex. Quartzo-feldspathic gneisses are the major component of the Xilinhot complex, including biotite-plagioclase gneiss, two mica-plagioclase gneiss, and sericite-plagioclase gneiss (Li et al. 2016a, b). The magmatic rocks of the Xilinhot block are exposed discontinuously along the northern margin of the Lixin Fault (Fig. 1), the northern boundary of the Solonker (Sun et al. 2013a, b).

The Baolidao arc is composed of variably deformed, metaluminous to weakly peraluminous, hornblende-bearing gabbroic diorite, quartz diorite, tonalite and granodiorite (IMBGMR 1991; Chen et al. 2000). U-Pb zircon ages indicate that the bulk of the Baolidao rocks were emplaced in Late Carboniferous time at circa 310 Ma (Xiao et al. 2003). Contemporaneous volcano-sedimentary rocks to the north formed in island arc and back arc settings (Nan and Guo 1992). Ophiolites and blueschists between Sunid Zouqi and Xilinhot (Fig. 1) occur as lenses in north dipping Carboniferous and Early Permian clastic sediments, and are overlain unconformably by Upper Permian conglomerates (Wang and Liu 1986). The Precambrian rocks outcrop in the Xilinhot and Sonid Zuoqi regionals belong to blocks that were accreted to the margin of the CAOB and incorporated into the subduction-accretion complex before the terminal closure of the central Asian ocean and formation of the Solonker suture (Xiao et al. 2003).

Sample petrology and analytical methods

Our study areas are located at the Erdaojing and Tulinkai (Figs. 1, 2) of the central segment of Inner Mongolia. In total, one metamorphic diorite sample and five schist samples were collected in the autumn of 2013 and the summer of 2014. U-Pb zircon dating analysis were performed on the igneous and schist samples. Sample locations (Fig. 2a, b) are shown in Table 1. Specifically, Fig. 3a is the stratum section of Ondor Sum complex and Carboniferous strata which outcrop in the Tulinkai area. The Ondor Sum schist with the fault contact relationship to the Carboniferous strata consist of the limestone within thin bedding sandstone, and the strata are domain dip to north. The detail location of the albite schist sample (Sample PM101TW21) are showing in this section (Fig. 3a), and the sample is very fresh and medium- to coarse- grained. To the north, the chromite-bearing quartzite as the lens body outcrop the contact between the schist and phyllite (sample D03) (Fig. 3c). A metamorphic diorite dike (Sample D02) intruded into the

Table 1 Summary of sample numbers and sample locations

Sample number	Description	Dating method	Latitude (°N)	Longitude (°E)	Data source
D02	Diorite	U-Pb zircon	42.27°	112.46°	This study
D03	Phyllite	U-Pb zircon	42.26°	112.55°	This study
D10	Chlorite-sericite schist	U-Pb zircon	43.31°	113.40°	This study
D11	Quartz schist	U-Pb zircon	43.24°	113.31°	This study
PM101TW21-1	Albite schist	U-Pb zircon	42.24°	112.52°	This study
PM101TW21-2	Albite schist	U-Pb zircon	42.24°	112.52°	This study

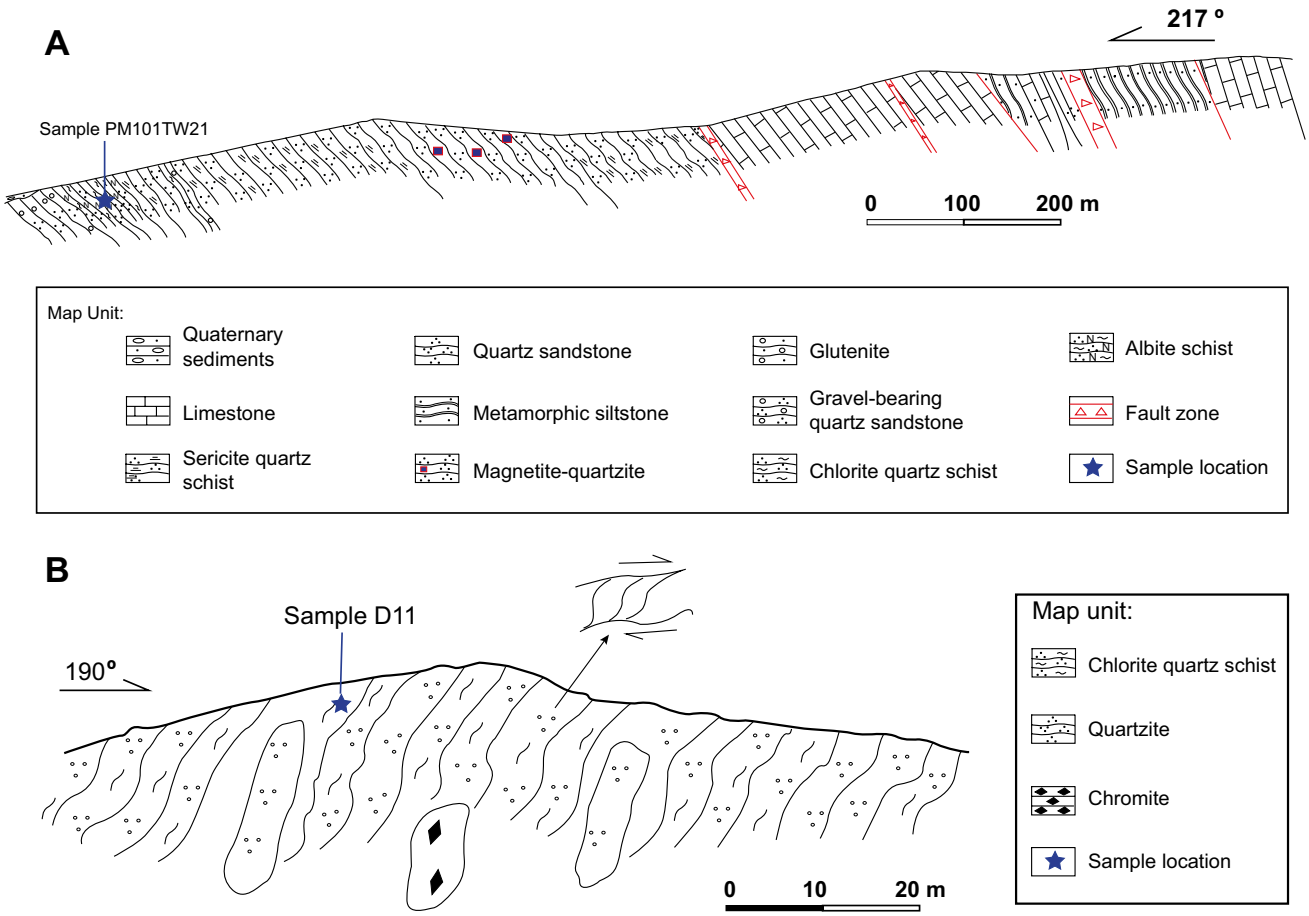

Fig. 3 The stratum sections of the Ondor Sum complex and Carboniferous strata which outcrop in the Tulinkai area (**a**), and Erdaojing metamorphic rocks that outcrop in the Erdaojing area (**b**)

Tulinkai Ultra-mafic rocks, but the occurrence of the contact relationships is discontinuous and the bedrock outcrop is scattered (Fig. 4a). Also, Fig. 3b is a simple stratum section of Erdaojing complex which outcrops in the Erdaojing area, the right lateral shear is developed across the metamorphic complex. The quartz schist (Sample D11) usually clip the chromite-bearing quartzite (Fig. 4d) as the lens body. To the west, the chlorite-sericite schist (Sample D10) is unconformity contact the upper volcanic rocks with the thin interbed of crust of weathering (Fig. 4b).

Sample petrology

Chlorite-sericite schist (Sample D10) The lower-medium grade metamorphic schist retains a fine greywacke to siltstone-like sedimentary texture and is mostly composed of clasts, which was collected from a weakly foliated metamorphic complex at the Erdaojing area (Fig. 4b). The basic mineralogical assemblage of this schist sample is 40% quartz, 60% chlorite + sericite. Accessory minerals include a small amount of limonite, tourmalines and zircon. The monocrystalline quartz and albite clasts are typically

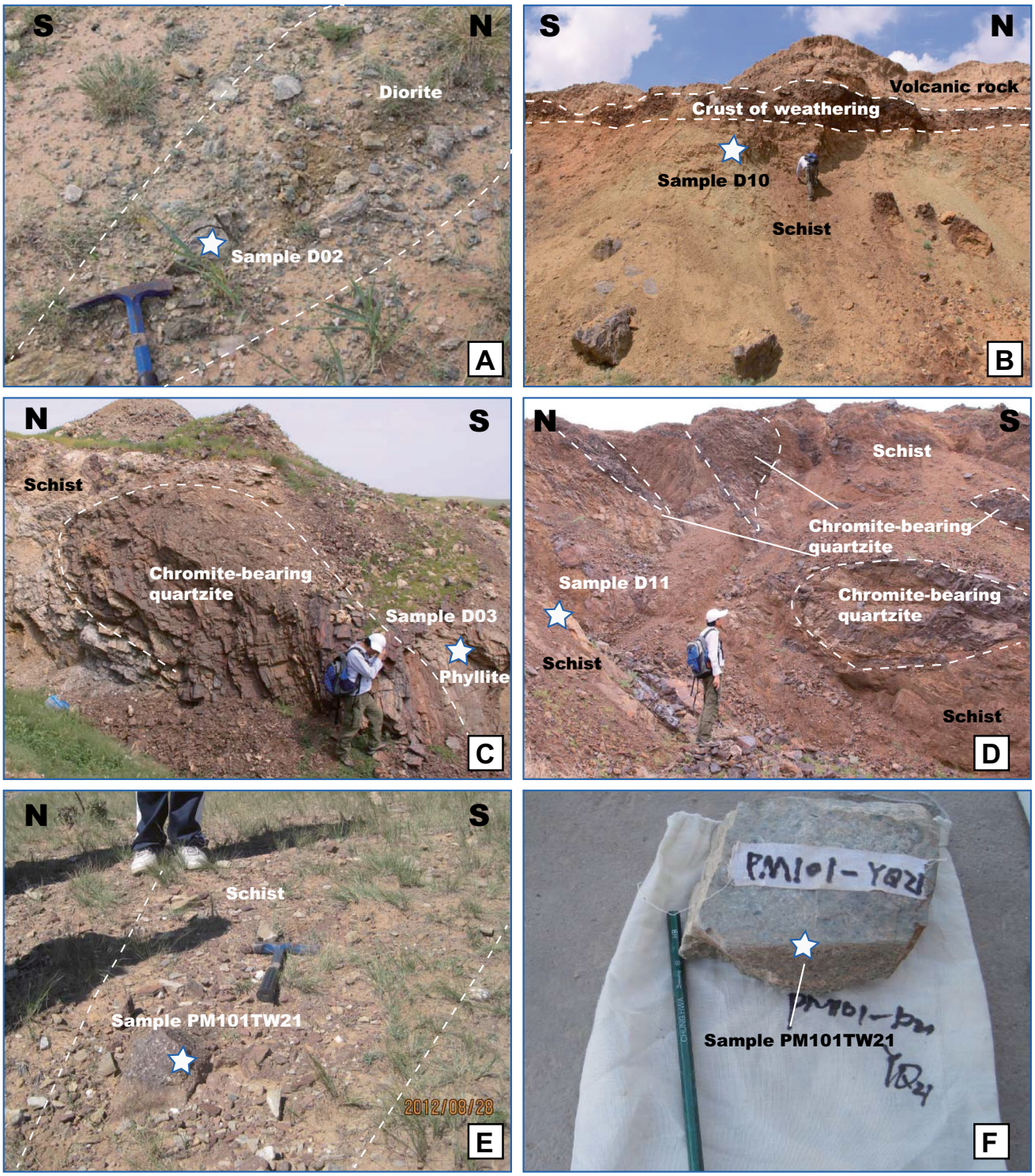

Fig. 4 Photographs of selected features of dated samples in this study

subhedral to euhrdral finer grained ranging from 0.02 to 0.20 mm in diameter. The aligned chlorites and sericites are typically scaly, averaging <0.1 mm in size. This chlorite-sericite schist is penetratively deformed by the development of schistosity. The foliation is defined by a minor amount of eclongated quartz grains bounded by foliation-parallel sericite (Fig. 5a), which is largely recrystallized and carry large quantities of chlorite or other platy minerals.

Quartz schist (Sample D11) The lower-medium grade metamorphic schist retains a fine greywacke to

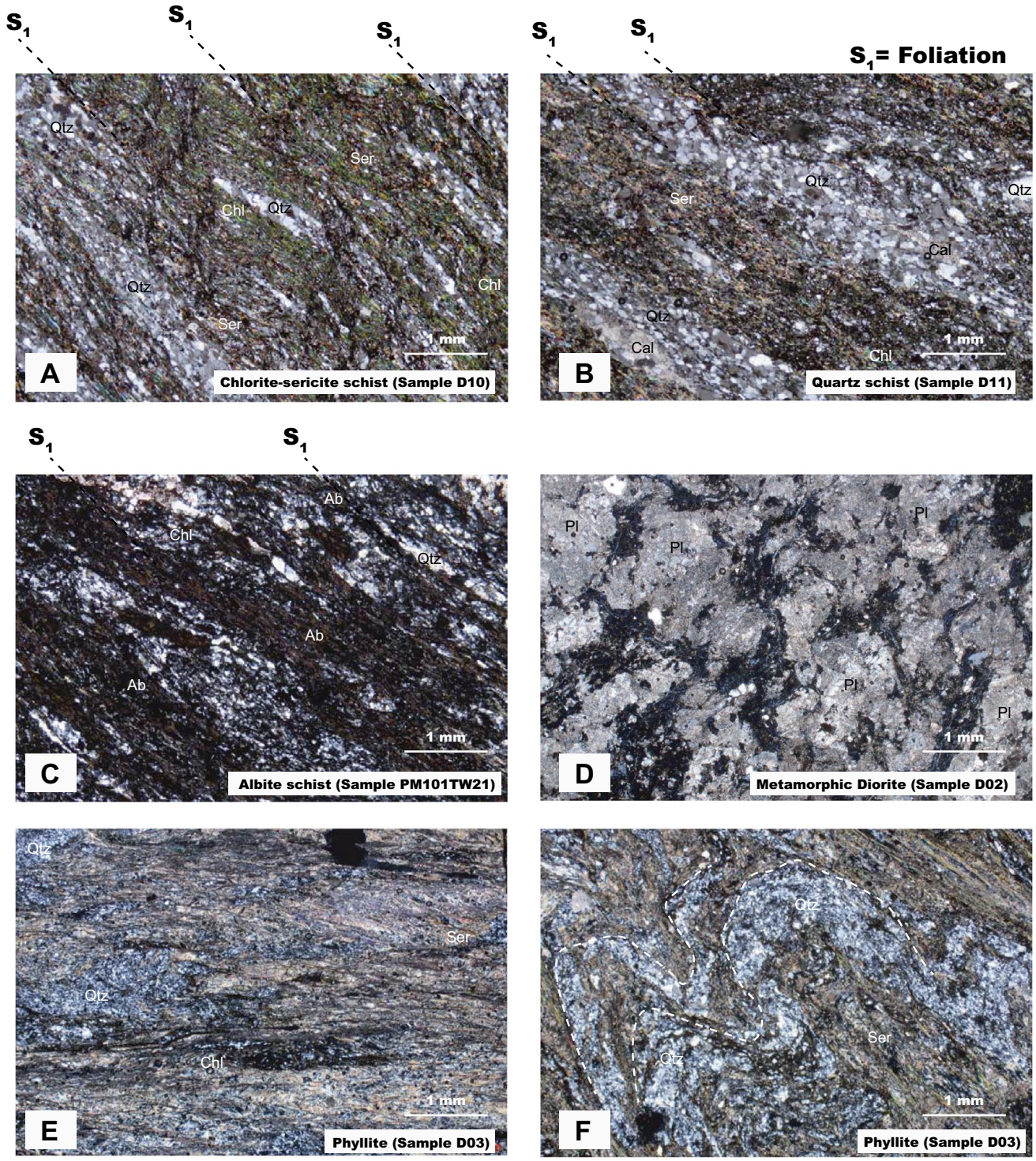

Fig. 5 Photomicrographs under plane polarized light showing the features of dated samples in this study. *Qtz* quartz, *Pl* plagioclase, *Chl* chlorite, *Cal* calcites, *Ab* albite, *Ser* sericite

siltstone-like sedimentary texture and is mostly composed of clasts, which was collected from a weakly foliated metamorphic complex at the Erdaojing area (Fig. 4d). The basic mineralogical assemblage of this schist sample is 75% quartz, 15% chlorite + sericite, 10% calcite. Accessory minerals include a small amount of tourmalines and zircon grains. The monocrystalline quartzes are typically subhedral to euhrdral finer grained ranging from 0.02 to 0.20 mm

in diameter. The aligned chlorites and sericites are typically scaly, averaging <0.1 mm in size. The calcite is typically subhedral to euhrdral finer grained ranging from 0.02 to 0.25 mm in diameter. This schist is penetratively deformed by the development of schistosity. The foliation is defined by a minor amount of eclongated quartz and calcite grains bounded by foliation-parallel sericite, which is also largely recrystallized and carry large quantities of chlorite or other platy minerals (Fig. 5b).

Albite schist (Sample PM101TW21) The Sample PM101TW21-1 and Sample PM101TW21-2 are a same sample collected from a weakly foliated metamorphic complex at the Tulinkai area (Fig. 4e, f). However, two different color zircons (pink for Sample PM101TW21-1 and purple for Sample PM101TW21-2) are found from this sample, therefore, we divided it into two parts and give them different sample number. These lower-medium grade metamorphic schists are medium- to coarse- foliated, which is lightly recrystallized but do not carry large quantities of mica or other platy minerals. The foliations are characterized by alternating darker and lighter colored bands. These schist samples consist of albite (75%), quartz (5%), chlorite (20%). The albites and rare quartzs are typically subhedral to euhrdral finer grained ranging from 0.1 to 0.2 mm in diameter, whereas the aligned chlorites are typically scaly and averaging <0.1 mm in size. Accessory minerals include a small amount of apatite and zircon (Fig. 5c).

Phyllite (Sample D03) The lower-grade metamorphic phyllite retains a fine greywacke to siltstone-like sedimentary texture and is mostly composed of clasts, which was collected from a weakly foliated metamorphic complex at the Tulinkai area (Fig. 4c). The basic mineralogical assemblage of this phyllite sample is 65% quartz + felspar, 35% chlorite + sericite, and rare calcite minerals. Accessory minerals include a small amount of zircons. The monocrystalline felsic minerals are typically subhedral to euhrdral finer grained ranging from 0.05 to 0.15 mm in diameter. The aligned chlorites and sericites are typically scaly, averaging <0.2 mm in size. The calcite is typically subhedral to euhrdral finer grained ranging from 0.02 to 0.4 mm in diameter. The foliation is defined by a minor amount of eclongated quartz and calcite grains bounded by foliation-parallel sericite, which is also largely recrystallized and carry large quantities of chlorite or other platy minerals (Fig. 5e, f).

Metamorphic diorite (Sample D02) This sample was collected from the Tulinkai area of the Ondor Sum complex (Fig. 4a). The diorite intruded into the ultramafic–mafic rocks. The basic mineralogical assemblage of this slightly metamorphic diorite sample is ca. 95% plagioclase, 5% melanocratic minerals (biotite and amphibole), and rare quartz minerals. The monocrystalline plagioclase minerals are typically subhedral to euhrdral finer grained ranging from 0.2 to 1.0 mm in diameter. The quartz minerals are typically euhrdral finer grained ranging from 0.05 to 0.35 mm in diameter. The sample shows the characteristic of obviously broken (Fig. 5d).

Analytical methods

All samples were collected from medium grained, with each sample weighing ~5 kg. Once samples collected, the schist samples were sent to the Institute of Hebei Regional Geology and Mineral Survey in Langfang, Hebei Province, for mineral separation. The samples were first crushed to pass a 60 mesh (250 μm) sieve. Manual washing with water and then alcohol was performed carefully for multiple aliquots of the crushed material to get the denser component of various grain sizes. An electromagnetometer was then used to remove magnetic minerals. Heavy liquid separation was used to concentrate heavy minerals, and the remaining non-zircon minerals were picked out by hand under a binocular, leaving only zircon grains in the sample. The zircon grains were mounted randomly in epoxy resin and polished close to one-third of individual grain diameters. Sample mounts were photographed in reflected and transmitted light. In order to guide laser ablation isotope analysis, grain growth structures were later depicted as cathodoluminescence (CL) images (Fig. 6). CL imaging was employed to investigate the rim-core relationships. For grains with cores and rims, we analyzed only the rims, as their ages record the most recent thermal events.

It is believed that at least 60 randomly selected grains should be measured to reduce the probability of missing one population comprising >5% of the total at a 95% significance level based on the standard binomial probability formula (Dodson et al. 1988). Both statements refer to the analysis of concordant ages. In this study, we aimed at analyzing at least 75 grains from each sample. Simultaneous analyses of U-Pb of detrital-zircon grains from 5 samples and one diorite sample were carried out at the Isotopic Laboratory, Tianjin Institute of Geology and Mineral Resources using an Agilent 7500a multicollector–inductively coupled plasma–mass spectrometer (MC-ICP-MS) and a Neptune MC-ICP-MS equipped with a 193-nm excimer ArF laser-ablation system. Each analysis was composed of an ~30 s background measure ment with laser off and a 60 s measurement of peak intensities. The ablation pits varied at 40, 50, and 60 μm in diameter, which depended on the size of sample grains, and at ~30–40 μm in depth. The ablated material was carried in helium into the Q-ICP-MS and MC-ICP-MS for simultaneous determination of U-Pb age. The analytical method used in this study follows Li et al. (2009).

Standard zircon 91,500 was employed to correct for mass bias affecting $^{207}Pb/^{206}Pb$, $^{206}Pb/^{238}U$, $^{207}Pb/^{235}U$

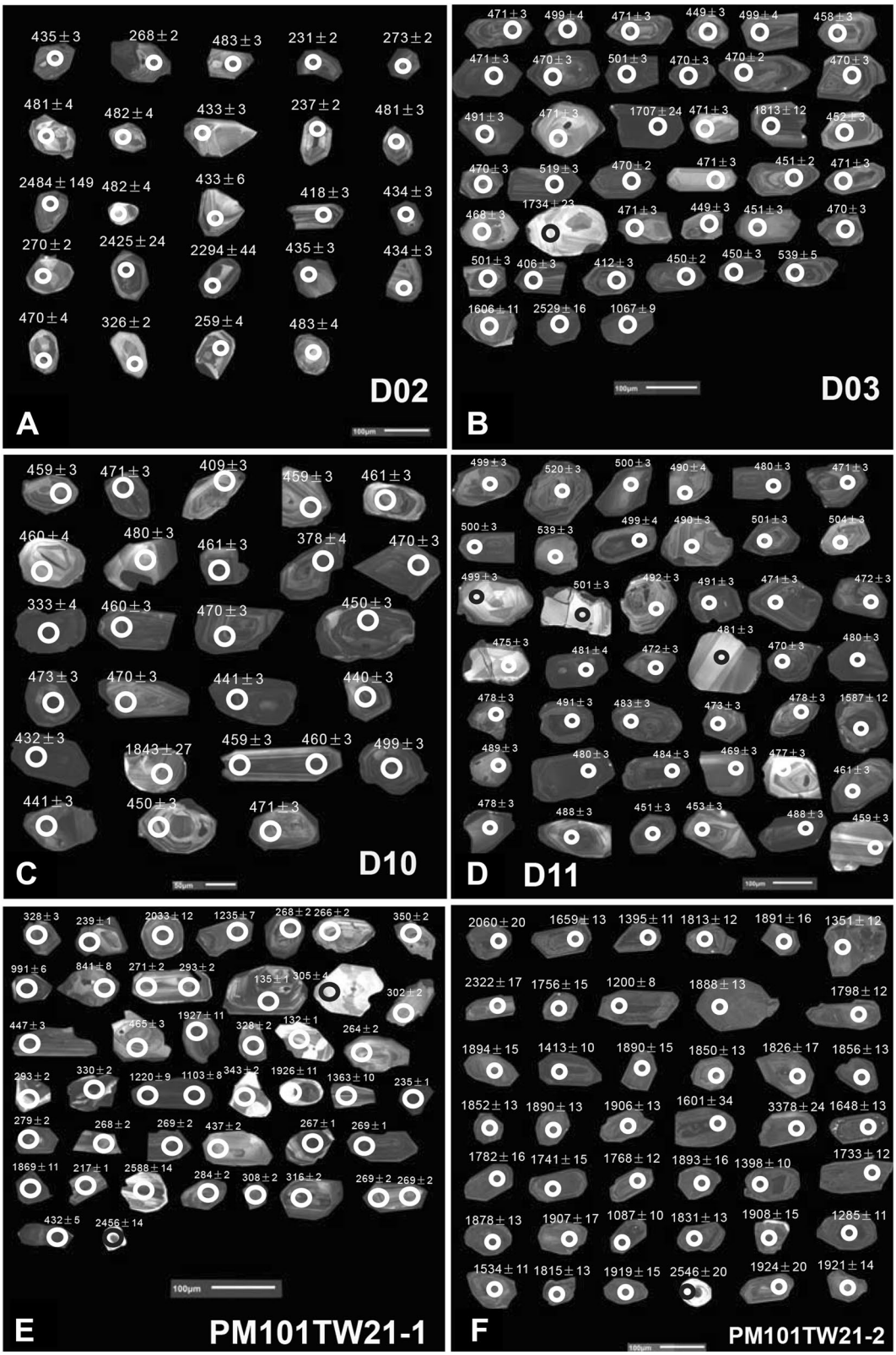

Fig. 6 Representative cathodoluminescence (CL) images of zircons dated in this study. *Black circles* are analyzed spots for U-Pb dating. The *numerals* are ages in Ma. *Scale bar* in each applies showing in all panels

($^{235}U = {}^{238}U/137.88$), and $^{208}Pb/^{232}Th$ ratios. NIST SRM 610 glass was used for concentration information and the U/Th ratio determination. The fractionation correction and results were calculated using GLITTER 4.0 (Macquarie University), and common Pb was corrected following the method described by Andersen (2002). The analytical data for U-Pb zircon dating are shown in Appendix Data. The total age probability density distribution of each sample was calculated by assuming a Gaussian error distribution for each single age and its respective 1σ error. Single age probability density distributions were summed to obtain the probability density distribution of the sample, and then normalized by the number of total analyses of each sample. The interpreted U/Pb ages are based on $^{206}Pb^*/^{238}U$ for grains younger than 1.0 Ga and $^{207}Pb^*/^{206}Pb^*$ for grains older than 1.0 Ga, with uncertainties both at the 1σ level. The concordia plots used a log–log scale in order to adequately visualize the entire age spectrum of a sample in a single plot. The unlikeliness that errors of each of the two isotope ratios reach simultaneously their maximum value has been taken into account by drawing error ellipses based on a 95% confidence level (2σ).

Results of U-Pb dating

The remaining ages are shown on U–Pb concordia diagrams and relative age-probability diagrams generated using Isoplot 4 (Ludwig 2008). The interpreted ages of zircon grains are shown on the relative age probability diagrams (Fig. 7) and $^{207}Pb/^{235}U$-$^{206}Pb/^{238}U$ concordia diagram (Fig. 8). Age-probability diagrams show each age and its uncertainty (for measurement error only) as a normal distribution, and sum all ages from a sample into a single probability density function.

Chlorite-sericite schist (Sample D10) Zircon crystals extracted from this sample are mostly euhedral, 100 zircon grains were analyzed, of which 87 passed the concordance filters (Fig. 7a). U-Pb dating indicates that major age populations lie in the range of 420–504 Ma, with the major age peak centered at ca. 461 Ma and ca. 475 Ma, respectively (Fig. 7a). A single zircon grain with a U-Pb age of ca. 420 Ma is the youngest zircon age of this sample. Also, two other single zircon grains with the U-Pb ages of ca. 1843 Ma and ca. 1846 Ma are the oldest zircon ages of this sample.

Quartz schist (Sample D11) Zircon crystals extracted from this sample are mostly euhedral, 100 zircon grains were analyzed, of which 100 passed the concordance filters (Fig. 7b). U-Pb dating indicates that major age populations lie in the range of 447–504 Ma, with the major age peak centered at ca. 471 Ma and ca. 451 Ma, respectively (Fig. 7b). Two single zircon grains with a U-Pb age of ca. 398 Ma and ca. 418 Ma are the youngest zircon ages of this sample. Also, two other single zircon grains with the U-Pb ages of ca. 1587 Ma and ca. 1965 Ma are the oldest zircon ages of this sample. Additional ages of ca. 520–539 Ma are source from the western extension of the Baolidao Arc, as the existence of the magmatic record in the Hadaaobao pluton of the Siziwangqi area.

Albite schist (Sample PM101TW21-1) Pink zircon crystals extracted from the sample are mostly euhedral. 60 zircon grains of sample PM101TW21-1 were analyzed, of which 39 passed the concordance filters (Fig. 7c). U-Pb dating indicates that major age populations lie in the range of 264-–269 Ma, with the major age peak centered at ca. 265 Ma and ca. 630 Ma, respectively (Fig. 7c). A single zircon grain with a U-Pb age of ca. 239 Ma is the youngest zircon age of this sample. The rest of the zircon grains yielded ages from ca. 991 Ma to ca. 2588 Ma without any obvious age clustering. Also, the single zircon grain with the U-Pb age of ca. 2588 Ma is the oldest zircon age of this sample.

Albite schist (Sample PM101TW21-2) Purple zircon crystals extracted from the sample are mostly euhedral. 100 zircon grains of sample PM101TW21-2 were analyzed, of which 96 passed the concordance filters (Fig. 7d). U-Pb dating indicates that major age populations lie in the range of 1043 Ma–2546 Ma, with the major age peak centered at ca. 1850 Ma and ca. 2200 Ma, respectively (Fig. 7d). A single zircon grain with a U-Pb age of ca. 1043 Ma is the youngest zircon age of this sample. Also, two single zircon grains with the U-Pb age of ca. 3378 Ma and ca. 3617 Ma are the oldest zircon ages of this sample.

Phyllite (Sample D03) Zircon crystals extracted from this sample are mostly euhedral, 100 zircon grains were analyzed, of which 89 passed the concordance filters (Fig. 7e). U-Pb dating indicates that major age populations lie in the range of 272 Ma-500 Ma, with the major age peak centered at ca. 472 Ma (Fig. 7e). One single zircon grain with a U-Pb age of ca. 272 Ma is the youngest zircon age of this sample. Also, two other single zircon grains with the U-Pb ages of ca. 3054 Ma and ca. 3131 Ma are the oldest zircon ages of this sample.

Metamorphic diorite (Sample D02) Zircon in this sample displays oscillatory zonation (Fig. 8). In total, 34 zircon grains were analyzed, with each grain sampled at one spot. Among the analyzed grains, 31 spots were collected from the zircon rims, which yield two age peaks at ca. 434.2 Ma and ca. 482.0 Ma (Fig. 8). The cores of the rest of the three grains yielded ages of ca. 2484 Ma, ca. 2425 Ma, ca. 2294 Ma, respectively (Fig. 8). One single zircon grain with a U-Pb age of ca. 237 Ma is the youngest zircon age of this sample. The wide range of zircon ages is likely a result of incorporation of older wall rock into the ascending magma from which the diorite sample dated in this study

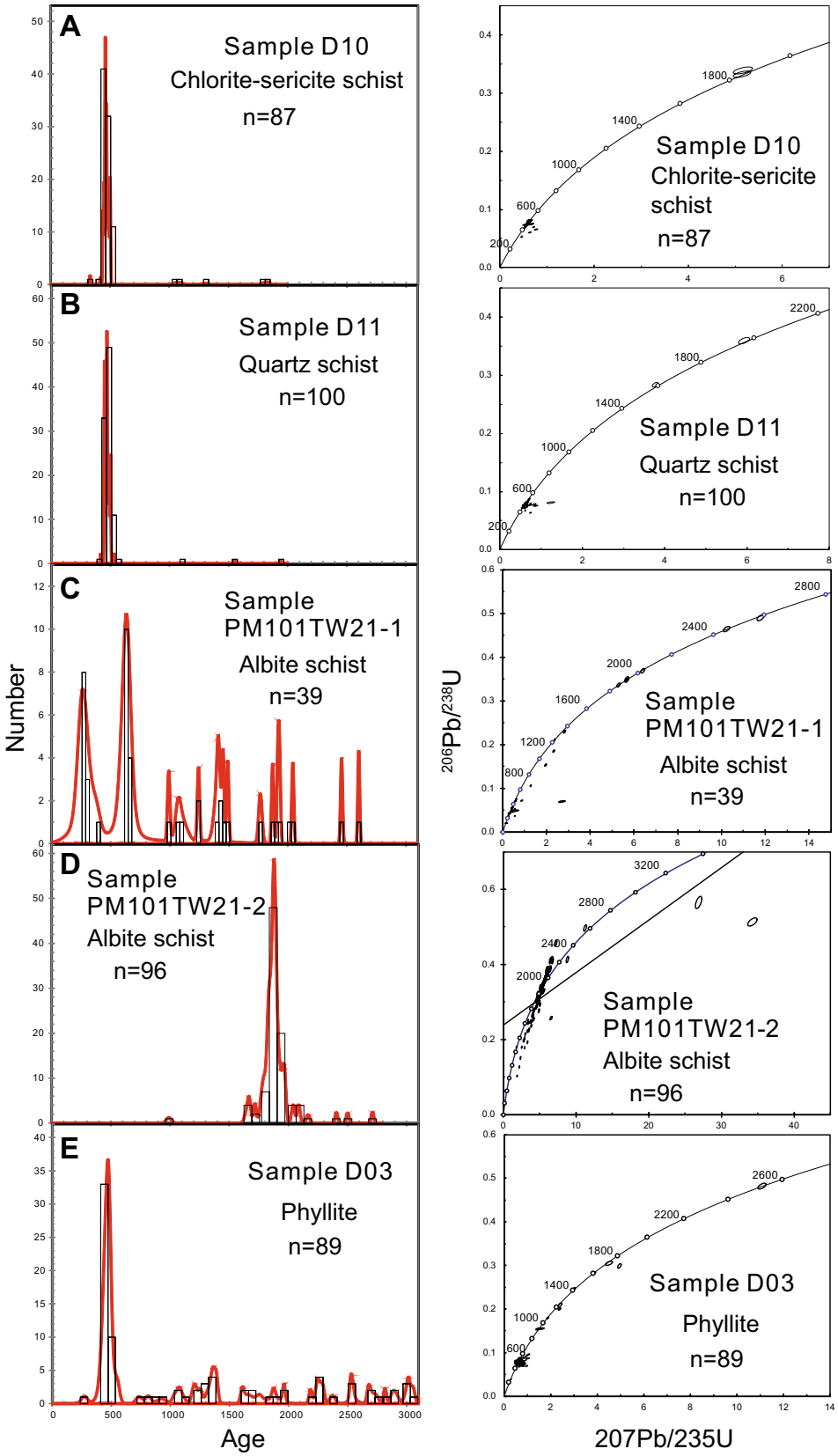

Fig. 7 Relative probability plots of detrital zircon U-Pb ages and zircon $^{207}Pb/^{235}U$-$^{206}Pb/^{238}U$ concordia diagrams for the para metamorphic rocks from this study

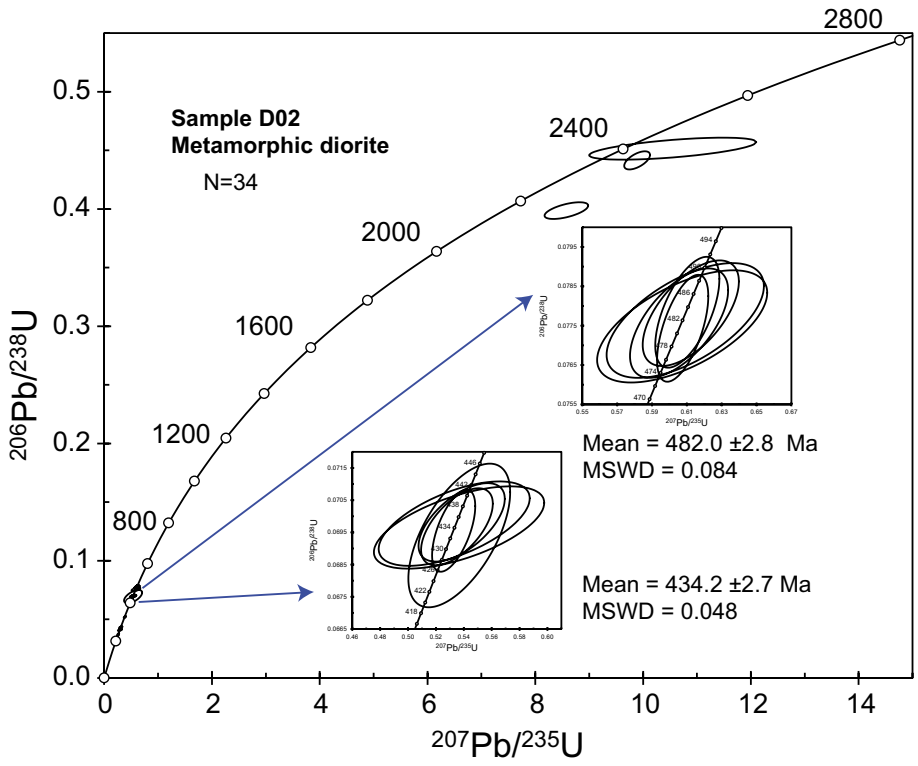

Fig. 8 Zircon $^{207}Pb/^{235}U$-$^{206}Pb/^{238}U$ concordia diagrams of metamorphic diorite sample (D02). *MSWD* mean square of weighted deviates

was derived. Thus, we interpret the younger rim age of ca. 434.2 Ma to represent the emplacement age of the dated diorite rock sample and the older core ages to represent the ages of inherited zircon dating of the diorite sample can be found in Appendix Data.

Discussion and conclusions

Provenance blocks of the Ondor Sum and Erdaojing complexes

Provenance analysis of Paleozoic metasedimentary complex along the Tulinkai and Erdaojing areas could provide an important insight into the role of major tectonic units as sedimentary provenance blocks during the evolution of the Paleo-Asian Ocean. Their relative contributions can be identified and defined by their characteristic age probability density distributions (Fig. 7).

The Bainaimiao arc located in the northern margin of the North China Craton to the south of the Ondor Sum complex, while the Baolidao arc to the north of the Erdaojing complex represent the most likely provenance blocks due to their close geographic location to the study region. Other provenance blocks such as the Siberian craton, Tarim craton, Gondwana-derived fragments within the eastern CAOB, and a Pan-African orogenic block (Songliao block) located in northeast China (Zhou et al. 2012) are less likely to have influenced the sedimentary system in the study region and will only be briefly discussed here. A detailed geochronological summary and discussion of most of these provenance blocks have been provided by Rojas-Agramonte et al. (2011, and references therein). As pointed out by Rojas-Agramonte et al. (2011), Gondwana fragments are generally characterized by a Pan-African age peak (650–550 Ma) and a Mesoproterozoic age gap (~1.75–1.0 Ga). The Siberian craton is characterized by a larger population of Archean to Early Paleoproterozoic ages (Rojas-Agramonte et al. 2011). Zircon U-Pb ages originating from the North China Craton generally range from ~3.8 to ~1.6 Ga, with major age peaks at 2.8–2.6, 2.4–2.35, and 2.1–1.85 Ga. For details see Fig. 9.

Our Erdaojing schist samples (sample D10 and sample D11) located in the Erdaojing complex are dominated by ca. 451 Ma, ca. 461 Ma, ca. 471 Ma and ca. 501 Ma zircon ages (Fig. 9), also, four other zircon grains with the U-Pb ages of ca. 1587 Ma, ca. 1843 Ma, ca. 1846 Ma and ca. 1965 Ma are detected from the age spectrum of these two samples. The former can be related to the Baolidao arc rocks in the north, whereas the latter can be related to the Proterozoic arc exposed in the crystalline basement complex of the Xilinhot Complex in the north (Sun et al. 2013a, b; Xu et al. 2014; Li et al. 2014; Wu et al. 2016). The absence of > 2.0 Ga zircons in these samples and a paucity of ages between 1.8 and 2.0 Ma indicate that the North China Craton is an unlikely source.

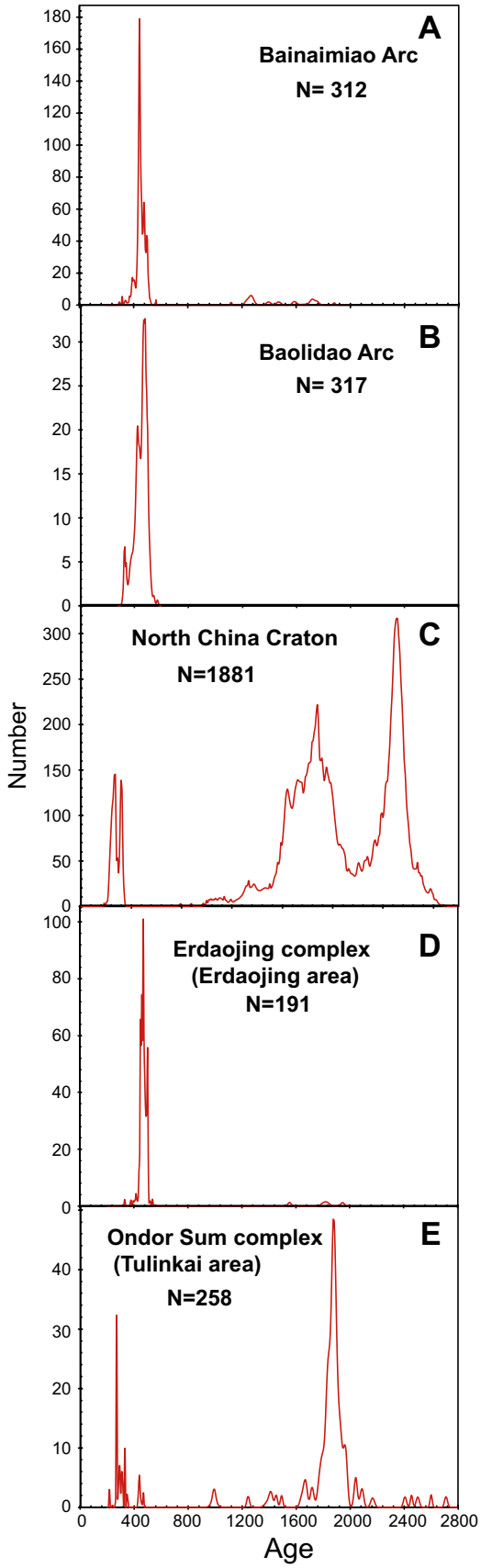

Fig. 9 Relative probability plot of igneous and metamorphic zircons from the Bainaimiao Arc, Baolidao Arc, North China Craton, Erdaojing complex, and Ondor Sum complex (Tulinkai area). For data sources see Zhou et al. (2009), Rojas-Agramonte et al. (2011), Li et al. (2012), Chu et al. (2013), Eizenhöfer et al. 2014, 2015, Liu et al. (2015a), Song et al. (2015), Li et al. (2016), Wu et al. (2016) and therein references

The sedimentary rock suite is characteristic of a higher quartzose but less detrital content compared with the volcanic rock suite. These observations suggest short transport distances from the major source regions and the sedimentary basins, with a certain degree of sedimentary reworking.

Our Tulinkai metamorphic rock samples located in the Ondor Sum complex are dominated by ca. 269 Ma and ca. 1875 Ma zircon ages (Fig. 9). The Paleoproterozoic age peaks (~2497 and ~1844 Ma) detected in this study region are similar to those from the North China Craton (e.g., Darby and Gehrels 2006). The Siberian craton is unlikely to have contributed to the study region. The Tarim Craton reveals a very heterogeneous age distribution with a distinct Neoproterozoic population (~788 Ma), neither of which is observed in the study area. Recently, Ge et al. (2013) reported abundant 2.5 and 1.85 Ga ages, similar to those of the North China Craton. As pointed out by Rojas-Agramonte et al. (2011), Gondwanan fragments are generally characterized by a Pan-African age peak (650–550 Ma) and a Mesoproterozoic age gap (~1.75–1.0 Ga). These age peak and gap are absent in the analyzed samples in this study. They, thus, are not considered as provenance sources of the study region. Also, e.g., Zhou et al. (2012) and Han et al. (2012) proposed that the Erguna, Xing'an, Jiamusi-Khanka, and Songliao blocks in northeast China have Pan-African basement and represent fragments that rifted from northern Gondwana, and may have influenced sedimentary systems in the region during Late Paleozoic. Taking into account the proximity to the study region, the North China Craton might be identified as a significant provider of sedimentary detritus to the Tulinkai metamorphic complex.

Therefore, other source terranes need to be considered to explain the dominant occurrence of Early and Late Paleozoic age populations (~436 and ~269 Ma, respectively) detected in the study area. An Early Paleozoic arc along the northern margin of North China Craton existed (Xiao et al. 2003), termed the Bainaimiao arc by Jian et al. (2008, 2010) and Wu et al. (2016). Early Paleozoic activity and collision with the Hunshandake microcontinent along the Ondor Sum Subduction-Accretion Complex were recently reported (Xiao et al. 2003; Shi et al. 2013; Xu et al. 2013). Phengites in blueschists from the Ondor Sum Subduction-Accretion Complex gave Ar/Ar ages of 453.2 ± 1.8 and 449.4 ± 1.8 Ma (De Jong et al. 2006). Zircons from a biotite-plagioclase gneiss sample collected from the Xilinhot

complex yielded upper and lower intercept ages of 437 ± 3 and 316 ± 3 Ma, respectively (Shi et al. 2003). Additionally, Cope et al. (2005) considered that a continental arc existed along the northern margin of the North China Craton from ~400 to ~275 Ma based on detrital zircon analysis of Carboniferous to Permian nonmarine strata. These lines of evidence suggest that the Early and Late Paleozoic zircons in the arc basins originated most likely from a major Paleozoic provenance terrane along the northern margin of North China Craton. Also, the provenance of clastic sediments within a single depositional system can shift dramatically over a short period of time simply as a function of the shifting of sediment delivery systems such as rivers. A dramatic demonstration of this sort of geologic history is given by Dumitru et al. (2013).

In summary, we consider that at least two different provenance terranes contributed to the Erdaojing and Tulinkai areas located in the Erdaojing complex to the north and the Ondor Sum complex to the south, respectively: (1) the Precambrian basement of the North China Craton and Paleozoic Bainaimiao Arc along the northern margin of North China in the south are the provenance rocks of the schists in the Tulinkai area, and (2) the Precambrian basement of the Xilinhot complex and Paleozoic Baolidao arc in the north are the provenance rocks of the schists in the Erdaojing area. So, the Erdaojing complex to the north and the Ondor Sum complex to the south belong to the different tectonic units, which sourced from the different material of the remnants of oceanic crust. Based on our regional data analysis, we infer that the existence of the ocean between the the Erdaojing complex and the Ondor Sum complex in the Early Paleozoic in accordance with the results of this study. The youngest zircon age of 239 Ma from the albite schist sample located in the Tulinkai area indicates that the depositional age and formation age of the Onder Sum complex are less than 239 Ma and the Ocean should still exist at ca. 239 Ma, so the accurate age of the Onder Sum complex is the key to constrain the closure time of the ocean basin. But it remains unclear whether it was a wide ocean, a narrow ocean, a relict marginal basin, or a Red Sea-type basin.

Timing of the closure of the Paleo-Asian Ocean

A number of Late Paleozoic zircon ages in the Ondor Sum complex to the south may also have been contributed to the arc basins by the active Northern Accretionary Orogen (Jian et al. 2008, 2010; Wu et al. 2016) during the final stages of ocean closure. However, their contribution to the Late Permian age population in the Linxi basin would be indistinguishable from those of the Southern Accretionary Orogen (Jian et al. 2008, 2010; Eizenhöfer et al. 2014; Wu et al. 2016). Furthermore, the detrital zircon age spectrum of the Ondor Sum Complex to the south in this study is dominated by the Precambrian and Late Paleozoic ages of the North China Craton and the Paleozoic ages of the Southern Accretionary Orogen (e.g., Bainaimiao Arc). Shi et al. (2003) suggested that Carboniferous ages should commonly occur within the Northern Accretionary Orogen (e.g., in the Xilinhot Complex).

Eizenhöfer et al. (2014) reported that an andesitic pyroclastic rock in the southern shoreline of the Xar Moron River formed between the Early and Middle Triassic, which was interpreted as the timing of latest volcanic activity related to the southward subduction of the Paleo-Asian Oceanic lithosphere. Also, an undeformed felsic dike intruding the Middle Permian Huangganglian Formation between the Early Triassic and Middle Triassic is interpreted to have recorded a period of latest magmatic activity and thus giving a constraint on the minimum depositional age of the Middle Permian strata (Eizenhöfer et al. 2014). The dominant age peaks in both igneous rocks, however, are located in the Early Triassic (240–250 Ma). Note that magmatic zircons from a biotite-plagioclase schist and an intrusive syncollisional granite of the Shuangjing Complex located along the northern banks of the Xar Moron River yielded ages of 298 ± 2 and 272 ± 2 Ma, respectively, suggesting that the final closure of the Paleo-Asian ocean has occurred at some time after 298 ± 2 and 272 ± 2 Ma, not in the Early Paleozoic (e.g., Li et al. 2007, 2011; Y. L.).

The existence of ocean floor in the Permian in western Inner Mongolia is suggested (Shang 2004; Jian et al. 2010; Li et al. 2011, 2014). A recent paleomagnetic study indicates that the existing ocean was a small remnant sea in the Late Paleozoic after the closure of Paleo-Asian Ocean in the Late Devonian (Zhao et al. 2013). There is a substantial body of evidence indicating that the final suturing of the Solonker zone occurred between the Late Permian and earliest Triassic (Xiao et al. 2003, 2009a, b; Miao et al. 2008; Jian et al. 2010; Li et al. 2011, 2014), which may be related to the closure of the Permian oceanic basin in western Inner Mongolia (Li et al. 2011). Specifically, the 234 ± 7 Ma zircon U–Pb age from Halatu post-collisional granite (Chen et al. 2009) and the 222 ± 4 Ma zircon U–Pb age from Sonid Zuoqi A type granites (Shi et al. 2007) then record the post-collisional relaxation after the final suturing of the Solonker zone. In additional, Li et al. (2014) suggested that the final suturing of the Solonker zone occurred from 269 to 231 Ma according to their geochronology and geochemistry data. The youngest major age peak observed in the Ondor Sum Complex metasedimentary rock samples in this study is at ~265 Ma (a single zircon age of ~239 Ma is the youngest age of the samples), which defines the maximum depositional age of sedimentary rocks in the arc basins (Dickinson and Gehrels 2009; Dumitru et al. 2010). So, the still existence of ocean at ca. 239 Ma is suggested

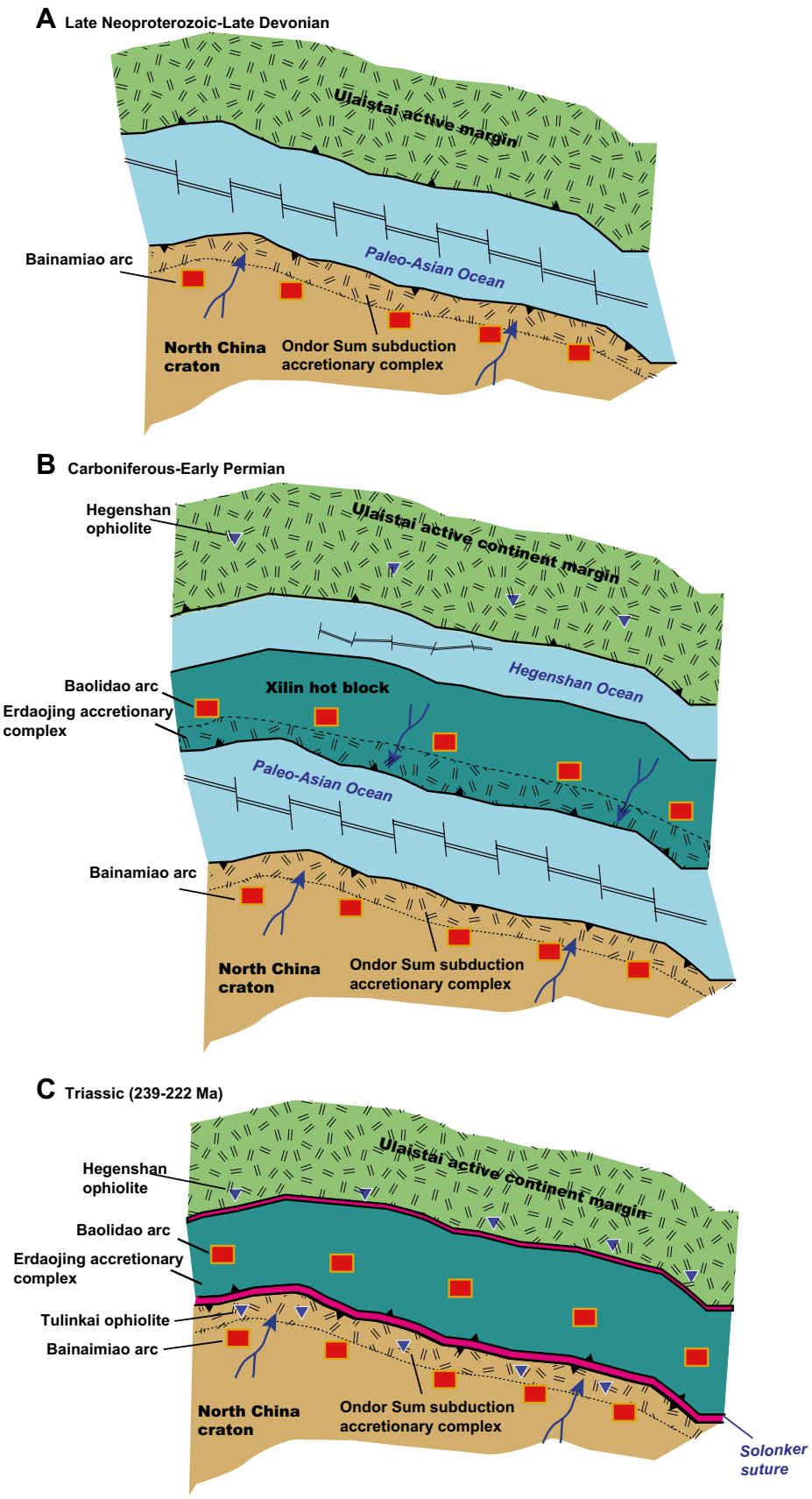

Fig. 10 Models for the Late Precambrian to Late Paleozoic geologic history of Xing'an-Mongolia Orogenic Belt in the eastern CAOB that conforms to our present understanding of the Palezo-Asian Ocean. Note that the scale is relatively and changes between panels. See text for details

in this study. In this study, one single zircon grain with a U-Pb age of ca. 237 Ma is the youngest zircon age of the dated diorite sample. Because there is no information on the geochemistry of this diorite dike, its origin is uncertain.

Taken together, our new data suggest that the final closure of the Paleo- Asian Ocean along the Solonker Suture Zone most likely occurred in the period between 239 and 222 Ma. Also, previous published data from other areas in vicinity of the region required that the Solonker Suture Zone developed in the Late Paleozoic or Triassic (e.g., Xiao et al. 2003, 2009a, b; Li et al. (2006); Windley et al. 2007; Jian et al. 2008, 2010), in accordance with the result of this study.

Late Neoproterozoic-Late Paleozoic tectonic evolution of eastern CAOB

Based on the data collected from this study and the regional published works, we propose a self-consistent tectonic model for the Late Neoproterozoic to Late Paleozoic geologic history of Xing'an-Mongolia Orogenic Belt in the eastern CAOB that conforms to our present understanding of the Palezo-Asian Ocean (Fig. 10). There was an Ulan arc (Xiao et al. 2003) to the north of the northern margin of the North China Craton within the Paleo-Asian Ocean in the Late Neoproterozoic. On the southern margins of the Ulan arc, the Ondor Sum accretionary complex was developed (Xiao et al. 2013; Xu et al. 2013). The southward subduction of the Paleo-Asian Ocean started from the Ordovician and create the Early Paleozoic Bainaimiao arc within the northern margin of the North China Craton (Fig. 10a). The sediments of Precambrian detrital zircon grains in the Ondor Sum accretionary complex derived from the North China Craton (Fig. 10a), also, the Bainaimiao arc is the source of the Early Paleozoic zircon grains. The blocks of Precambrian gneiss at Xilinhot block rifted from the Siberian Craton that were then accreted from the south, and the Baolidao island arc was attached to the collage in the Late Carboniferous (Fig. 10b). The Hegenshan ophiolite was developed in the southern segment of the Ulaistai active margin is evidence for the occurrence of the narrow Hegenshan Ocean northward subduction (Fig. 10b). The sediments of Precambrian detrital zircon in the Erdaojing accretionary complex derived from the Xilinhot block, also, the Baolidao arc is the source of the Paleozoic zircon grains (Fig. 10b). Our detrital zircon U-Pb age data allow us to infer the still existence of Paleo-Asian ocean before ca. 239 Ma. A ~222 Ma A-type granite that outcrop Sonid Zuoqi (Shi et al. 2007) record the post-collisional relaxation, represents that the final closure of the Paleo-Asian Ocean should have occurred after ca. 239 Ma but before ca. 222 Ma along the Solonker suture zone (Fig. 10c).

Acknowledgements We thank Professor Xiao Wenjiao, Professor John Wakabayashi and other three anonymous reviewers for their very constructive reviews that led to significant improvement of the original manuscript. This work was supported by the China University of Geosciences (Beijing), a grant from the Institute of Geological Survey, China University of Geosciences (Beijing). The detail project numbers of the China Geological Survey Program re Nos. 1212011120700, DD20160045, and 1212010510506.

References

Andersen T (2002) Correction of common lead in U-Pb analyses that do not report ^{204}Pb. Chem Geol 192:59–79

Badarch G, Dickson Cunningham W, Windley BF (2002) A new terrane subdivision for Mongolia: implications for the Phanerozoic crustal growth of Central Asia. J Asian Earth Sci 21(1):87–110

Cawood PA, Kröner A, Collins WJ, Kusky TM, Mooney WD, Windley BF (2009) Accretionary orogens through Earth history. Geol Soc Lond Spec Publ 318(1):1–36

Chen B, Jahn BM, Wilde S, Xu B (2000) Two contrasting Paleozoic magmatic belts in northern Inner Mongolia, China: petrogenesis and tectonic implications. Tectonophysics 328(1–2):157–182

Chen B, Jahn BM, Tian W (2009) Evolution of the Solonker suture zone: Constraints fromzircon U–Pb ages, Hf isotopic ratios and whole rock Nd–Sr isotope compositions of subduction- and collision-related magmas and forearc sediments. J Asian Earth Sci 34:245–257

Chu H, Zhang JR, Wei CJ, Wang HC, and Ren YW (2013) A new interpretation of the tectonic setting and age of meta-basic volcanics in the Ondor Sum Group, Inner Mongolia. Chin Sci Bull Kexue Tongbao 58, 3580–3587.

Cope T, Ritts BD, Darby BJ, Fildani A, Graham SA (2005) Late Paleozoic sedimentation on the northern margin of the North China block: implications for regional tectonics and climate change. Int Geol Rev 47(3):270–296

Darby BJ, Gehrels G (2006) Detrital zircon reference for the North China block. J Asian Earth Sci 26(6):637–648

De Jong K, Xiao WJ, Windley BF, Masago H, Lo CH (2006) Ordovician Ar^{40}/Ar^{39} phengite ages from the blueschist-facies Ondor Sum subduction-accretion complex (Inner Mongolia) and implications for the Early Paleozoic history of continental blocks in China and adjacent areas. Am J Sci 306(10):799–845

Dickinson WR, Gehrels GE (2009) U-Pb ages of detrital zircons in Jurassic eolian and associated sandstones of the Colorado Plateau: evidence for transcontinental dispersal and intraregional recycling of sediment. Earth Planet Sci Lett 288(1):115–125

Dodson MH, Compston W, Williams IS, Wilson JF (1988) A search for ancient detrital zircons in Zimbabwean sediments. J Geol Soc 145(6):977–983

Dumitru TA, Wakabayashi J, Wright JE, Wooden JL (2010) Early cretaceous transition from nonaccretionary behavior to strongly accretionary behavior within the Franciscan subduction complex. Tectonics 29(5)

Dumitru TA, Ernst WG, Wright JE, Wooden JL, Wells RE, Farmer LP, Kent AJR, Graham SA (2013) Eocene extension in Idaho generated massive sediment floods into the Franciscan trench and into the Tyee, Great Valley, and Green River basins. Geology 41(2):187–190

Eizenhöfer PR, Zhao GC, Zhang J, Sun M (2014) Final closure of the Paleo-Asian Ocean along the Solonker Suture

Zone: constraints from geochronological and geochemical data of Permian volcanic and sedimentary rocks. Tectonics 33:441–463

Eizenhöfer PR, Zhao GC, Zhang J, Han YG, Hou WZ, Liu DX, Wang B (2015) Geochemical characteristics of the Permian basins and their provenances across the Solonker Suture Zone: assessment of net crustal growth during the closure of the Palaeo-Asian Ocean. Lithos 224–225:240–255

Ge R, Zhu W, Wu H, Zheng B (2013) Zircon U-Pb ages and Lu-Hf isotopes of Paleoproterozoic metasedimentary rocks in the Korla Complex, NW China: Implications for metamorphic zircon formation and geological evolution of the Tarim Craton. Precambrian Res 231:1–18

Han GQ, Liu YJ, Neubauer F, Jin W, Genser J, Ren SM, Li W, Wen QB, Zhao YL, Liang CY (2012) LA-ICP-MS U-Pb dating and Hf isotopic compositions of detrital zircons from the Permian sandstones in Da Xing'an Mountains, NE China: New evidence for the eastern extension of the Erenhot-Hegenshan suture zone. J Asian Earth Sci 49:249–271

Haughton PDW, Todd SP, Morton AC (1991) Sedimentary provenance studies. Geol Soc London Spec Publ 57(1):1–11

Hsu¨ KJ, Wang Q, Li J, Hao J (1991) Geologic evolution of the Neimonides: A working hypothesis. Eclogae Geol Helv 84:1–31

Hu X, Xu C, Niu S (1990) Evolution of the Early Paleozoic Continental Margin in Northern Margin of the North China Platform (in Chinese with English abstract). Peking Univ. Press, Beijing, pp 216

IMBGMR (Inner Mongolian Bureau of Geology and Mineral Resources) (1991) Regional Geology of Inner Mongolian Autonomous Region. Geological Publishing House, Beijing (Chinese with English abstract)

Jahn BM, Wu FY, Chen B (2000) Massive granitoid generation in Central Asia: Nd isotope evidence and implication for continental growth in the Phanerozoic. Episodes 23:82–92

Jahn BM (2004) The Central Asian Orogenic Belt and growth of the continental crust in the Phanerozoic, in Aspects of the Tectonic Evolution of China, edited by J. Malpas et al. Geol Soc Lond Spec Publ 226:73–100

Jian P, Liu DY, Kröner A, Windley BF, Shi YR, Zhang FQ, Shi GH, Miao LC, Zhang W, Zhang Q, Zhang LQ, Ren JS (2008) Timescale of an Early to Mid-Paleozoic orogenic cycle of the long lived Central Asian Orogenic Belt, Inner Mongolia of China: implications for continental growth. Lithos 101(3–4):233–259

Jian P, Liu DY, Kröner A, Windley BF, Shi YR, Zhang W, Zhang FQ, Shi GH, Miao LC, Zhang LQ, Tomurhuu D (2010) Evolution of a Permian intraoceanic arc–trench system in the Solonker suture zone, Central Asian Orogenic Belt, China and Mongolia. Lithos 118:169–190

Jian P, Kröner A, Windley BF, Shi Y, Zhang W, Zhang L, Yang W (2012) Carboniferous and cretaceous mafic–ultramafic massifs in Inner Mongolia (China): a SHRIMP zircon and geochemical study of the previously presumed integral "Hegenshan ophiolite". Lithos 142–143:48–66

Kröner A, Windley BF, Badarch G, Tomurtogoo O, Hegner E, Jahn BM, Gruschka S, Khain EV, Demoux A, Wingate MTD (2007) Accretionary growth and crust formation in the Central Asian Orogenic Belt and comparison with the Arabian-Nubian shield. Geol Soc Am Mem 200:181–209

Lehmann J, Schulmann K, Lexa O, Corsini M, Kröner A, Stipska P, Tomurhuu D, Otgonbator D (2010) Structural constraints on the evolution of the Central Asian Orogenic Belt in SW Mongolia. Am J Sci 310(7):575–628

Li JY (1986) The principal characteristics of pillow lavas in the Linxi district and its tectonic significance. Bull Shenyang Inst Geol Min Res Chin Acad Geol Sci 14:1637–1641.

Li JY (1987) A preliminary study on the Paleo-suture between Siberian and Sino-Korean plates in Eastern Nei Mongolia. Chin Sci Bull 32:65–74

Li XH, Li ZX, Wingate MTD, Chung SL, Liu Y, Lin GC, Li WX (2006) Geochemistry of the 755 Ma Mundine Well dyke swarm, northwestern Australia: part of a Neoproterozoic mantle superplume beneath Rodinia? Precambrian Res 146:1–15

Li JY, Gao LM, Sun GH, Li YP, and Wang YB (2007) Shuangjingzi middle Triassic syn-collisional crust-derived granite in the east Inner Mongolia and its constraint on the timing of collision between Siberian and Sino-Korean paleo-plates. Acta Petrol Sin 23(3):565–582.

Li, XH, Y. Liu, Q.L. Li, C.H. Guo, and K. R. Chamberlain (2009) Precise determination of Phanerozoic zircon Pb/Pb age by multicollector SIMS without external standardization. Geochem Geophys Geosyst 10:Q04010. doi:10.1029/2009GC002400

Li YL, Zhou HW, Brouwer FM, Xiao WJ, Zhong ZQ, Wijbrans JR (2011) Late Carboniferous–Middle Permian arc/forearc-related basin in Central Asian Orogenic Belt: insights from the petrology and geochemistry of the Shuangjing Schist in Inner Mongolia, China. Isl Arc 20(4):535–549.

Li CD, Ran H, Zhao LG, Wang HC, Zhang K, Xu YW, Gu YC, Zhang YQ (2012) LA-MC-ICPMS U-Pb geochronology of zircons from the Ondor Sum Group and its tectonic significance. Acta Petrol Sin 28(11):3705–3714 (in Chinese with English abstract)

Li YL, Zhou HW, Brouwe FM, Xiao WJ, Wijbrans JR, Zhao JH, Zhong ZQ, Liu HF (2014) Nature and timing of the Solonker suture of the Central Asian Orogenic Belt: insights from geochronology and geochemistry of basic intrusions in the Xilin Gol Complex, Inner Mongolia, China. Int J Earth Sci Geol Rundsch 103:41–60

Li YL, Brouwer FM, Xiao WJ, Wang KL, Lee YH, Luo BJ, Su YP, Zheng JP (2016a) Subduction-related metasomatic mantle source in the eastern Central Asian Orogenic Belt: Evidence from amphibolites in the Xilingol Complex, Inner Mongolia, China. Gandwana Res. doi:10.1016/j.gr.2015.11.015

Li YL, Brouwer FM, Xiao WJ, Zheng JP (2016b) Late Devonian to Early Carboniferous arc-related magmatism in the Baolidao arc, Inner Mongolia, China: significance for southward accretion of the eastern Central Asian Orogenic Belt. Geol Soc Am Bull. doi:10.1130/B31511.1

Li HY, Zhou ZG, Li PJ, Zhang D, Liu CF, Zhao XQ, Chen LZ, Gu CN, Lin TT, and Hu MM (2016c) Ordovician intrusive rocks from the eastern Central Asian Orogenic Belt in Northeast China: chronology and implications for bidirectional subduction of the early Palaeozoic Palaeo-Asian Ocean. Int Geol Rev 58(10):1175–1195.

Lin W, Faure M, Nomade S, Shang QH, Renne PR (2008) Permian-Triassic amalgamation of Asia: Insights from Northeast China sutures and their place in the final collision of North China and Siberia. C R Geosci 340(2–3):190–201.

Liu DY, Jian P, Zhang Q, Zhang FQ, Shi YR, Shi GH, Zhang FQ, Tao H (2003) SHRIMP dating of Adakites in the Tulingkai Ophiolite, inner Mongolia: evidence for the Early Paleozoic Subduction. Acta Geol Sinica 77(3):317–327 (**Chinese with English abstract**)

Liu JF, Li JY, Chi XG, Zhao Z, Hu ZC, Feng QW (2012) Petrogenesis of middle Triassic post-collisional granite from Jiefangyingzi area, southeast Inner Mongolia: Constraint on the Triassic tectonic evolution of the north margin of the Sino-Korean paleoplate. J Asian Earth Sci 60:147–159

Liu CF, Wu C, Zhu Y, Zhou ZG, Jiang T, Liu WC, Li HY (2015) Late Paleozoic-Early Mesozoic magmatic history of the central Inner Mongolia, China: implications for the Tectonic Evolution of the Xing'an-Mongolia Orogenic Belt, southeastern segment of the

Central Asian Orogenic Belt. J Asian Earth Sci. doi:10.1016/j.jseaes.2015.09.011

Liu YJ., Li WM, Feng ZQ, Wen QB, Neubauer F, Liang CY (2016) A review of the Paleozoic tectonics in the eastern part of Central Asian Orogenic Belt. Gondwana Res. doi:10.1016/j.gr.2016.03.013

Ludwig KR (2008) Isoplot version 3.7, User's Manual. Berkeley Geochronology Center Special Publication 4

Miao LC, Fan WM, Liu DY, Zhang FQ, Shi YR, Guo F (2008) Geochronology and geochemistry of the Hegenshan ophiolitic complex: Implications for late-stage tectonic evolution of the Inner Mongolia-Daxinganling Orogenic Belt, China. J Asian Earth Sci 32(5–6):348–370

Nan RS, Guo SZ (1992) Paleozoic Biostratigraphy and Palaeo-geography in the Geosynclinal region of Nei Mongol and Northeast China (in Chinese with English abstract). Geol Publ House, Beijing

Nozaka T, Liu Y (2002) Petrology of the Hegenshan ophiolite and its implication for the tectonic evolution of northern China. Earth Planet Sci Lett 202(1):89–104

Rojas-Agramonte Y, Kröner A, Demoux A, Xia X, Wang W, Donskaya T, Liu D, Sun M (2011) Detrital and xenocrystic zircon ages from Neoproterozoic to Palaeozoic arc terranes of Mongolia: Significance for the origin of crustal fragments in the Central Asian Orogenic Belt. Gondwana Res 19(3):751–763

Sengör AMC, Natal'in BA (1996) Paleotectonics of Asia: fragments of a synthesis. In: Yin A, Harrison M. (eds) The tectonic evolution of Asia. Cambridge University Press, Cambridge, pp 486–641

Şengör AMC, Natal'in BA, Burtman VS (1993) Evolution of the Altaid tectonic collage and Paleozoic crustal growth in Eurasia. Nature 364(6435):299–307

Shao JA (1989) Continental crust accretion and tectono-magmatic activity at the northern margin of the Sino-Korean plate. J Southeast Asian Earth Sci 3(1–4):57–62

Shang QH (2004) Occurrences of permian radiolarians in central and eastern Nei Mongol (Inner Mongolia) and their geological significance to the Northern China Orogen. Chin Sci Bull 49:2613–2619

Shen SZ, Zhang H, Shang QH, Li WZ (2006) Permian stratigraphy and correlation of Northeast China: a review. J Asian Earth Sci 26(3–4):304–326

Shi GH, Liu DY, Zhang FQ, Jian P, Miao LC, Shi YR, Tao H (2003) SHRIMP U-Pb zircon geochronology and its implications on the Xilin Gol Complex, Inner Mongolia, China. Chin Sci Bull 48(24):2742–2748

Shi YR, Liu DY, Zhang Q, Jian P, Zhang FQ, Miao LC, Zhang LQ (2007) SHRIMP U–Pb zircon dating of triassic A-type granites in Sonid Zuoqi, central Inner Mongolia, China, and its tectonic implications. Geol Bull China 26:183–189 (**in Chinese with English abstract**)

Shi GH, Faure M, Xu B, Zhao P, Chen Y (2013) Structural and kinematic analysis of the Early Paleozoic Ondor Sum-Hongqi mélange belt, eastern part of the Altaids (CAOB) in Inner Mongolia, China. J Asian Earth Sci 66:123–139

Song SS, Wang MM, Xu X, Wang C, Niu YL, Allen MB, Su L (2015) Ophiolites in the Xing'an-Inner Mongolia accretionary belt of the CAOB: implications for two cycles of seafloor spreading and accretionary orogenic events. Tectonics. doi:10.1002/2015TC003948

Sun LX, Ren BF, Zhao FQ, Gu YC, Li YF, Liu H (2013a) Zircon U-Pb dating and Hf isotopic compositions of the Mesoporterozoic granitic gneiss in Xilinhot Block,Inner Mongolia. Geol Bull China 32(2/3):327–340.

Sun LX, Zhao FQ, Wang HC, Ren BF, Peng SH, Teng F (2013b) Zircon U Pb Geochronology of Metabase rocks from the Baoyintu block in the Langshan area inner Mongolia and its tectonic significance. Acta Geol Sinica 87(2):197–207

Tang KD (1990) Tectonic development of Paleozoic foldbelts at the north margin of the Sino-Korean craton. Tectonics 9(2):249–260

Wang Q, Liu X (1986) Paleoplate tectonics between Cathaysia and Angaraland in Inner Mongolia of China. Tectonics 5:1073–1088

Wang F, Chen FK., Hou ZH, Peng P, Zhai MG (2009) Zircon ages and Sr-Nd-Hf isotopic composition of late Paleozoic granitoids in the Chongli-Chicheng area, northern margin of the North China block. Acta Petrol Sin 25, 3057–3074 (in Chinese with English abstract).

Windley BF, Alexeiev D, Xiao WJ, Kroner A, Badarch G (2007) Tectonic models for accretion of the Central Asian Orogenic Belt. J Geol Soc 164:31–47.

Wu FY, Sun DY, Li HM, Jahn BM, Wilde S (2002) A-type granites in northeastern China: age and geochemical constraints on their petrogenesis. Chem Geol 187(1–2):143–173

Wu FY, Zhao GC, Sun DY, Wilde SA, Yang JH (2007) The Hulan Group: its role in the evolution of the Central Asian Orogenic Belt of NE China. J Asian Earth Sci 30(3–4):542–556

Wu C, Jiang T, Liu CF, Liu WC (2014) Early Cretaceous A-type granites and Mo mineralization, Aershan area, eastern Inner Mongolia, Northeastern China: geochemical and Isotopic constraints. Int Geol Rev 56(11):1357–1376

Wu C, Jiang T, Liu WC, Zhang D, Zhou ZG (2015) Early Cretaceous adakitic granites and mineralization of the Yili porphyry Mo deposit in the Great Xing'an range: implications for the geodynamic evolution of northeastern China. Int Geol Rev 57(9–10):1152–1171

Wu C, Liu C, Zhu Y, Zhou ZG, Jiang T, Liu WC, Li HY (2016) Early Paleozoic magmatic history of the central Inner Mongolia, China: implications for the tectonic evolution of the Southeast Central Asian Orogenic Belt. Int J Earth Sci 105:1307–1327

Xiao WJ, Windley BF, Hao J, Zhai MG (2003) Accretion leading to collision and the Permian Solonker suture, Inner Mongolia, China: termination of the central Asian orogenic belt. Tectonics 22(6):1069

Xiao WJ, Windley BF, Huang BC, Han CM, Yuan C, Chen HL, Sun M, Sun S, Li JL (2009a) End-Permian to mid-Triassic termination of the accretionary processes of the southern Altaids: implications for the geodynamic evolution, Phanerozoic continental growth, and metallogeny of Central Asia. Int J Earth Sci 98(6):1189–1217

Xiao WJ et al (2009b) Paleozoic multiple subduction-accretion processes of the southern Altaids. Am J Sci 309:221–270

Xiao WJ, Huang BC, Han CM, Sun S, Li JL (2010) A review of the western part of the Altaids: a key to understanding the architecture of accretionary orogens. Gondwana Res 18(2–3):253–273

Xiao WJ, Windley BF, Allen MB, Han CM (2013) Paleozoic multiple accretionary and collisional tectonics of the Chinese Tianshan orogenic collage. Gondwana Res 23(4):1316–1341

Xiao WJ, Windley BF, Sun S, Li JL, Huang BC, Han CM, Yuan C, Sun M, Chen H (2015) A tale of amalgamation of three collage systems in the Permian-Middle Triassic in Central Asia: Oroclines, sutures and terminal accretion. Annu Rev Earth Planet Sci 43:477–507

Xu B, Charvet J, Zhang FQ (2001) Primary study on petrology and geochronology of the blueschist in Sonid Zuoqi, northern Inner Mongolia. Chin J Geol 36:424–434 (**in Chinese with English abstract**)

Xu B, Charvet J, Chen Y, Zhao P, Shi G (2013) Middle Paleozoic convergent orogenic belts in western Inner Mongolia (China): framework, kinematics, geochronology and implications for tectonic evolution of the Central Asian Orogenic Belt. Gondwana Res 23(4):1342–1364

Xu B, Zhao P, Bao QZ, Zhou YH, Wang YY, Luo ZW (2014) Preliminary study on the pre-Mesozoic tectonic unit division of the Xing-Meng Orogenic Belt (XMOB). Acta Petrol Sin 30:1841–1857 (in Chinese with English abstract)

Xu B, Zhao P, Wang YY, Liao W, Luo ZW, Bao QZ, Zhou YH (2015) The pre-Devonian tectonic framework of Xing'an-Mongolia orogenic belt (XMOB) in north China. J Asian Earth Sci 97:183–196

Yakubchuk A (2008) Re-deciphering the tectonic jigsaw puzzle of northern Eurasia. J Asian Earth Sci 32(2–4):82–101

Ye M, Zhang SH, Wu FY (1994) The classification of the Paleozoic tectonic units in the area crossed by Manzhouli-Suifenghe geoscience transect. J Chang Univ Earth Sci 24, 241–245 (**in Chinese with English abstract**)

Zhai M, Shao JA, Hao J, and Peng P (2003), Geological signature and possible position of the North China Block in the supercontinent Rodinia. Gondwana Res 6:171–183.

Zhang SH, Zhao Y, Song B, Yang ZY, Hu JM, Wu H (2007) Carboniferous granitic plutons from the northern margin of the North China block: implications for a late Palaeozoic active continental margin. J Geol Soc 164:451–463.

Zhang SH, Zhao Y, Kroner A, Liu XM, Xie LW, Chen FK (2009a) Early Permian plutons from the northern North China Block: Constraints on continental arc evolution and convergent margin magmatism related to the Central Asian Orogenic Belt. Int J Earth Sci 98(6):1441–1467

Zhang SH, Zhao Y, Liu XC, Liu DY, Chen F, Xie LW, Chen HH (2009b) Late Paleozoic to Early Mesozoic mafic-ultramafic complexes from the northern North China Block: constraints on the composition and evolution of the lithospheric mantle. Lithos 110:229–246

Zhang XH, Wilde S, Zhang HF, Tang YJ, Zhai MG (2009c) Geochemistry of hornblende gabbros from Sonidzuoqi, Inner Mongolia, North China: implications for magmatism during the final stage of suprasubduction-zone ophiolite formation. Int Geol Rev 51(4):345–373

Zhang J, Wei C, Chu H (2015) Blueschist metamorphism and its tectonic implication of Late Paleozoic-early Mesozoic metabasites in the mélange zones, central Inner Mongolia, China. J Asian Earth Sci 97:352–364

Zhao P, Chen Y, Xu B, Faure M, Shi G, Choulet F (2013). Did the Paleo-Asian Ocean between North China Block and Mongolia Block exist during the late Paleozoic? First paleomagnetic evidence from central-eastern Inner Mongolia, China. J Geophys Res Solid Earth 118:1873–1894

Zhou ZG, Zhang HF, Liu HL, Liu CF, Liu WC (2009). Zircon U–Pb dating of basic intrusions in Siziwangqi area middle Inner Mongolia, China. Acta Petrol Sin 25(6):1519–1528 (in Chinese with English abstract)

Zhou JB, Wilde SA, Zhang XZ, Liu FL, Liu JH (2012) Detrital zircons from phanerozoic rocks of the Songliao Block, NE China: Evidence and tectonic implications. J Asian Earth Sci 47:21–34